

# Electron Transfer at Liquid/Liquid Interfaces. The Effects of Ionic Adsorption, Electrolyte Concentration, and Spacer Length on the Reaction Rate

Biao Liu and Michael V. Mirkin\*

Department of Chemistry and Biochemistry, Queens College—CUNY, Flushing, New York 11367

Received: September 17, 2001; In Final Form: January 14, 2002

Several factors affecting the rate of heterogeneous electron transfer (ET) reactions at the nonpolarized interface between two immiscible electrolyte solutions (ITIES) were investigated by scanning electrochemical microscopy (SECM). The reactions between zinc porphyrin in organic phase and aqueous  $\text{Ru}(\text{CN})_6^{3/4-}$  or  $\text{Fe}(\text{CN})_6^{3/4-}$  redox species, which have previously served as model systems for probing the potential dependence of the ET rate constant, were used to investigate the effects of adsorption of a reactant and a potential-determining ion on ET rate at the interfaces between water and different organic solvents. It was demonstrated that the rate constant of an interfacial ET can be either potential-independent or potential-dependent under different experimental conditions. The same model experimental systems were used to probe the kinetics of long-range ET across a monolayer of phospholipid adsorbed at the ITIES. The results obtained with a family of phosphatidylserine lipids are compared to those previously obtained with synthetic phosphatidylcholine lipids. The extent of blocking effect of adsorbed lipids on interfacial ET was investigated at different pHs and also in the presence of calcium ions in the aqueous phase. The micrometer-sized domain formation in the monolayer was observed in the presence of divalent cations.

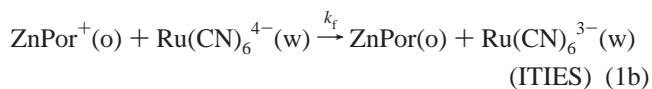
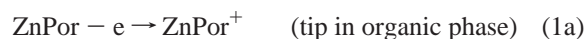
## Introduction

There has been a surge of activity in studies of electron transfer (ET) processes at the interface between two immiscible electrolyte solutions (ITIES) during the last several years. The kinetics of ET reactions between different aqueous and organic redox species have been measured.<sup>1</sup> Several research groups employed scanning electrochemical microscopy (SECM) to probe ET at the nonpolarizable<sup>2–8</sup> and polarizable<sup>9</sup> ITIES. Those studies identified the experimental conditions under which interfacial electron transfer can be probed and demonstrated that ET can be quantitatively separated from ion transfer processes. As expected from theory,<sup>10</sup> the studied reactions were found to be of the first order in both organic and aqueous redox species and the effective heterogeneous rate constants were strongly dependent on the difference between standard potentials of two redox couples ( $\Delta E^\circ$ ). Perhaps the most controversial point in this area is the contribution of the interfacial potential drop to the driving force for ET reactions.

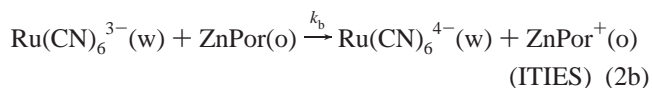
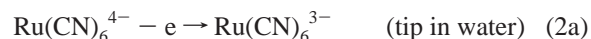
Most experimental data obtained at polarized<sup>9,11,12</sup> and nonpolarized ITIES<sup>3,6b,d,8</sup> supported the assumption that ET at the ITIES is driven by the potential drop across the interfacial boundary [for the ITIES this is the difference of Galvani potentials of the organic and aqueous phases ( $\Delta_w^0\varphi$ )]. Accordingly, the dependence of the ET rate constant on  $\Delta_w^0\varphi$  is expected to be exponential (Butler–Volmer equation) at lower overpotentials and to level off at much higher overpotentials.<sup>10</sup> However, the Butler–Volmer model (and Marcus theory) is applicable only if most of the interfacial voltage drops between the reacting redox moieties. This assumption is not highly plausible because the interfacial voltage drops mostly within the diffuse layer in organic phase.<sup>13</sup> According to a widely accepted three-layer model of the ITIES, the ET rate constant should be essentially potential-independent because the potential drop across the mixed-solvent layer separating aqueous and

organic redox species is small.<sup>14</sup> At the same time, the diffuse layer effect, similar to the Frumkin effect at metal electrodes, may result in either accumulation or depletion of a reactant species in the proximity of the phase boundary (mostly on the organic side<sup>14</sup>). Thus, the apparent rate constant is expected to depend on  $\Delta_w^0\varphi$  if the organic reactant is charged and to be essentially independent of  $\Delta_w^0\varphi$  when neutral organic species participate in the ET reaction.<sup>14c</sup>

These theoretical predictions have been corroborated only for one model experimental system, the reaction between zinc porphyrin (ZnPor) in organic phase and hexacyanorutinate in water. Both the forward (reaction 1b<sup>3b,c</sup>)



and reverse (reaction 2b<sup>7</sup>)



ET processes were investigated by SECM. In those experiments, the ultramicroelectrode (UME) tip was positioned in the top phase, which was either organic (Figure 1A) or aqueous (Figure 1B). The redox mediator contained in the top phase (either ZnPor or  $\text{Ru}(\text{CN})_6^{4-}$ ) was oxidized at the UME surface. When the tip approached the bottom liquid layer, the mediator was regenerated via interfacial bimolecular ET (either reaction 1b or 2b). The rate constants of reactions 1b and 2b were evaluated from the SECM tip current vs distance curves. To probe the

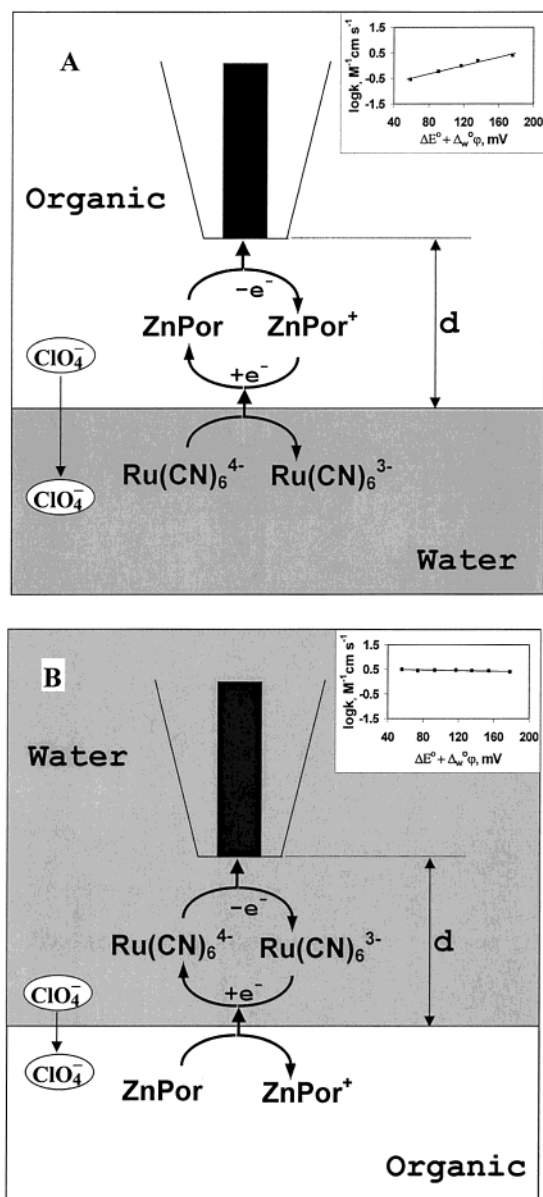


**Figure 1.** Schematic diagram of SECM measurements of the kinetics of ET between (a) ZnPor<sup>+</sup> in organic phase and Ru(CN)<sub>6</sub><sup>4-</sup> in aqueous phase and (b) ZnPor in organic phase and Ru(CN)<sub>6</sub><sup>3-</sup> in aqueous phase. The insets show the corresponding potential dependences of the rate constant from ref 3b (A) and 7 (B).

potential dependence of the rate constant,  $\Delta_w\phi$  was varied by changing the concentration of the common ion in the aqueous phase ( $[\text{ClO}_4^-]_w$ ).<sup>3b,7</sup> The potential drop across a nonpolarizable ITIES was shown to follow the Nernst–Donnan equation

$$\Delta_w\phi = \text{const} - S \log[\text{ClO}_4^-]_w \quad (3)$$

and the measured slope,  $S$ , was 56 mV/decade for nitrobenzene (NB) and 60 mV/decade for 1,2-dichloroethane (DCE) and benzene (BZ).<sup>3b,7</sup> For reaction 1b, the  $\log k_f$  vs  $\Delta_w\phi$  dependence was linear with a transfer coefficient,  $\alpha = 0.5$  (see inset in Figure 1A). Thus, it was proposed that the ET kinetics can be described by the Butler–Volmer model, and the driving force for the interfacial ET reaction is the sum of the  $\Delta_w\phi$  term and the difference of standard potentials of the organic and aqueous redox mediators:<sup>3b,c</sup>

$$\Delta G^\circ = -F(\Delta E^\circ + \Delta_w\phi) \quad (4)$$

It was suggested later,<sup>7</sup> that the observed dependence of the ET rate on  $\Delta_w\phi$  can also be explained by Schmickler’s model.<sup>14c</sup> Within the frame of that model, the increase in the  $k_f$  at more positive  $\Delta_w\phi$  is attributed to accumulation of ZnPor<sup>+</sup> at the interface rather than to increasing driving force for ET. Unlike forward reaction 1b, the electron acceptor in the reverse reaction 2b is anionic and the electron donor is a neutral species. The concentration of the neutral ZnPor at the interface is potential-independent. Since only a small fraction of the interfacial voltage drops within the aqueous diffuse layer, the effect of  $\Delta_w\phi$  on surface concentration of Ru(CN)<sub>6</sub><sup>3-</sup> is small. Accordingly, the  $k_b$  remained essentially constant within the limit of experimental error when the  $\Delta_w\phi$  was changed by about 120 mV (inset in Figure 1B). Similar results were obtained for three different organic solvents, i.e., BZ, NB, and DCE.<sup>7</sup>

One should notice, however, that no other potential-independent rate constants have been measured at either polarizable or nonpolarizable ITIES (the only exception is ref 15, where the kinetic analysis was complicated by the transfer of ferrocenium ion, which could occur simultaneously with ET). The rates of ET reactions involving such neutral organic reactants as 7,7,8,8-tetracyanoquinodimethane (TCNQ)<sup>6b,8</sup> or decamethylferrocene (DMFc)<sup>6c,7</sup> at nonpolarizable ITIES depended significantly on the  $\Delta_w\phi$  (though in the latter case the potential dependence was at variance with both Butler–Volmer and Marcus models). At a polarizable ITIES, the rate of ET reactions between neutral phthalocyanine complexes of lutetium or tin in organic phase and charged aqueous species also appeared potential-dependent, and the Butler–Volmer model was used for kinetic analysis.<sup>11a,b</sup> Recent spectroelectrochemical studies using neutral organic reactants (e.g., ferrocene)<sup>13,16</sup> have also showed some potential dependence of the interfacial ET rate constant. Here, we report more experiments aimed to clarify the origins of potential-independent kinetics of reaction 2b.

Another objective of this work is to compare the kinetics of long-range ET across monolayers of different phospholipids adsorbed at the ITIES. Our interest in studying ET across phospholipid films at the ITIES is 2-fold. First, this process is of fundamental importance for a number of biological systems.<sup>17</sup> On the other hand, by separating the electron donor and acceptor with a well-defined spacer one can slow the ET rate and carry out measurements at high overpotentials in order to check the ET theory.<sup>18</sup> ET can also be used as a yardstick to probe the properties of the interfacial film.<sup>19</sup> In this way, Delville et al.<sup>3d</sup> compared the rates of ET across the monolayers of saturated dipalmytoylphosphocholine and polyconjugated 2(3-(diphenylhexatrienyl)propanoyl)-1-hexadecanoyl-*sn*-glycero-3-phosphocholine lipids adsorbed at the water/benzene interface and showed that polyconjugated chains added to dipalmytoyl film behave as conducting wires increasing the overall ET rate. SECM imaging of mixed lipid films at the ITIES revealed the formation of micrometer-size domains.<sup>3d</sup> Separating ET reactants with a long-chain spacer can also increase the fraction of  $\Delta_w\phi$  dropping between them and in this way increase the potential dependence of the rate constant.

An earlier SECM study<sup>3c</sup> showed that adsorption of symmetric saturated lipids (1,2-dicacyl-*sn*-glycero-3-phosphocholine) with a different number of methylene groups in a hydrocarbon chain ( $n$ ) on the water/BZ interface results in a formation of a compact monolayer. The defect density in the film was too low to produce detectable feedback current. Although the redox reactants (i.e., ZnPor<sup>+</sup> in BZ and Fe(CN)<sub>6</sub><sup>4-</sup> in water) were separated by the lipid film and the rate of ET decreased markedly with the increasing length of the spacer,

the analysis of distance dependence of the rate constant suggested partial penetration of ZnPor<sup>+</sup> into the lipid layer. This prevented quantitative interpretation of the  $k_f$  vs  $n$  results.

Here we explore the possibility of improving the blocking properties of a spacer by using another family of saturated symmetric phospholipids, i.e., 1,2-diacyl-*sn*-glycero-3-phospho-L-serines. An interesting feature of phosphatidylserine films is that their structure can be easily and predictably changed. The liquid-expanded monolayers formed by these lipids at the ITIES at room temperature<sup>20</sup> undergo a sharp phase transition and become solid upon addition of a low concentration of a divalent cation (e.g., Ca<sup>2+</sup> or Mg<sup>2+</sup>).<sup>20b</sup> Such films are supposed to be tightly packed and may not be permeable to large porphyrin molecules.

### Experimental Section

**Chemicals.** 5,10,15,20-Tetraphenyl-21H,23H-porphine zinc (ZnPor), tetrabutylammonium tetraphenylborate (TBATPB), NaClO<sub>4</sub>, and NaCl from Aldrich (Milwaukee, WI), and Na<sub>4</sub>-Fe(CN)<sub>6</sub> (Fisher Scientific, Fair Lawn, NJ) were used as received. Na<sub>4</sub>Ru(CN)<sub>6</sub> was synthesized as reported previously,<sup>3b,21</sup> recrystallized several times from methanol/water and dried under vacuum overnight at 50 °C. Tetrahexylammonium perchlorate (THAClO<sub>4</sub>; Johnson Matthey, Ward Hill, MA) was recrystallized twice from an ethyl acetate:ether (9:1) mixture and dried under vacuum overnight at room temperature. Tetrabutylammonium chloride (TBACl), tetrabutylammonium hexafluorophosphate (TBAPF<sub>6</sub>), and nitrobenzene (>99%) were from Fluka Chemika, Switzerland. Benzene (spectrophotometric grade) and 1,2-dichloroethane (99.8% HPLC grade) were from Aldrich. All organic solutions were washed with a larger volume of Milli-Q water several times before measurements to remove impurities from the organic phase. All other chemicals were ACS reagent grade.

Chloroform solutions of symmetric saturated synthetic lipids (1,2-dicacyl-*sn*-glycero-3-phosphocholine and 1,2-dicacyl-*sn*-glycero-3-[phospho-L-serine]) with different numbers of methylene groups in a hydrocarbon chain ( $n = 10, 12, 16$ ; the abbreviations C-10, C-12, etc. will be used to designate different phospholipids) from Avanti Polar Lipids, Inc. (Alabaster, AL) were stored at -20 °C. Before an experiment, a flow of nitrogen was passed above a small volume (~40 μL) of phospholipid solution in chloroform for complete evaporation of solvent. The precipitated lipid was then redissolved in either BZ or DCE or NB to prepare a 500 μM stock solution, which also contained ZnPor and supporting electrolyte. The mixture of the lipid stock solution and BZ solution containing the same concentrations of ZnPor and THAClO<sub>4</sub> served as the organic phase.

**Electrodes and Electrochemical Cells.** A three-electrode setup was employed with a 12.5-μm-radius Pt ultramicroelectrode tip, a Pt wire as the counter electrode, and a Ag/AgCl reference electrode; all three electrodes were placed in the top liquid phase. The UME tip was rinsed with ethanol and water and then polished and dried before each measurement. When the top phase was organic, an ionic bridge containing a solution of NaCl and NaClO<sub>4</sub> (or TBACl) was placed between the Ag/AgCl reference electrode and organic solution.<sup>3b</sup>

To measure the rate of reaction 1b, the top phase contained a solution of 0.25 M THAClO<sub>4</sub>, 0.5 mM ZnPor, and 0–100 μM lipid in BZ or NB or DCE, and the bottom phase contained a solution of 7 mM of Na<sub>4</sub>Ru(CN)<sub>6</sub> or Na<sub>4</sub>Fe(CN)<sub>6</sub>, 0.1 M NaCl, and 0.01–2 M NaClO<sub>4</sub> or 5–100 mM TBACl. The organic solution was deaerated before each experiment. To measure the rate of reaction 2b, the top phase contained a 0.1 mM solution

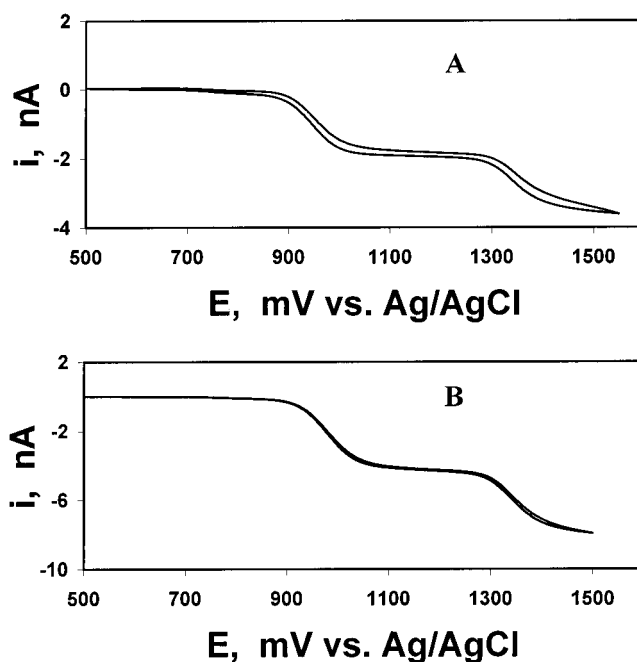


**Figure 2.** Steady-state voltammograms of 2 mM ZnPor at a 25-μm diameter Pt disk electrode in (A) NB and (B) DCE containing 25 mM TBAPF<sub>6</sub>. Scan rate was 5 mV/s.

of Na<sub>4</sub>Ru(CN)<sub>6</sub>, 0.1 M NaCl, and 0.01–2 M NaClO<sub>4</sub> or 5–100 mM TBACl; and the bottom (organic) phase contained a solution of 2 mM ZnPor, 1–100 mM THAClO<sub>4</sub>, or 10–200 mM TBAPF<sub>6</sub> in NB or DCE. The steady-state voltammograms of ZnPor in solutions containing TBA<sup>+</sup> (Figure 2) were very similar to those obtained previously in perchlorate solutions.<sup>3b,7</sup> The electrochemical cell designed to keep a lower density liquid phase (e.g., water) under a heavier liquid (e.g., DCE) was described previously.<sup>22</sup>

**SECM Apparatus and Procedure.** The SECM instrument was described previously.<sup>22,23</sup> Before SECM measurements, the tip electrode was positioned in the top phase. The tip was biased either at a potential corresponding to the plateau current of Ru(CN)<sub>6</sub><sup>4-</sup> oxidation in water or to the plateau current of the first oxidation wave of ZnPor in organic phase.

The approach curves were obtained by moving the tip toward the liquid/liquid interface and recording the tip current ( $i_T$ ) as a function of the tip/ITIES separation distance ( $d$ ). The coordinate of the liquid/liquid interface ( $d = 0$ ) was determined from the sharp change in  $i_T$  that occurred when the tip touched the ITIES.

The concentration of ZnPor in organic phase ( $\leq 5$  mM) was limited by its solubility. When an organic solvent was used as a bottom phase, the concentration of aqueous redox species was not higher than  $[\text{ZnPor}]_o/20$  to avoid diffusion limitations in the bottom layer.<sup>3,7</sup>

**Potential Drop across the ITIES.** In SECM measurements, a nonpolarizable ITIES is poised by the concentrations of the common ion providing a controllable driving force for the ET reaction.<sup>3</sup> The interfacial potential drop ( $\Delta_w^o\phi$ ) is governed by the ratio of common ion (i.e., ClO<sub>4</sub><sup>-</sup> or TBA<sup>+</sup>) concentration in the organic and aqueous phases (i.e.,  $[\text{ClO}_4^-]_o/[\text{ClO}_4^-]_w$  or  $[\text{TBA}^+]_o/[\text{TBA}^+]_w$ ). The  $\Delta_w^o\phi$  value was varied either by changing the concentration of the common ion in water (i.e.,  $[\text{ClO}_4^-]_w$  or  $[\text{TBA}^+]_w$ ) at a constant concentration of that ion in organic phase (typically, 10–100 mM), or vice versa, the common ion concentration was changed in the organic phase and kept constant in the aqueous phase. The relative values of  $\Delta_w^o\phi$  were obtained from cyclic voltammograms of either

**TABLE 1: Slope Values (*S*) for the Concentration Dependencies of  $\Delta_w^0\varphi$  Measured at the DCE/Water and NB/Water Interfaces**

concentration varied	organic solvent	<i>S</i> , mV/decade	reference
$[\text{ClO}_4^-]_w$	DCE	-59, -60	6c, 7
$[\text{ClO}_4^-]_o$	DCE	59, 65	6c, this work
$[\text{ClO}_4^-]_w$	NB	-56	7
$[\text{ClO}_4^-]_o$	NB	62	this work
$[\text{TBA}^+]_w$	DCE	59, 66	6c, this work
$[\text{TBA}^+]_o$	DCE	-61	this work
$[\text{TBA}^+]_w$	NB	60	this work
$[\text{TBA}^+]_o$	NB	-59	this work

ZnPor (Figure 2) or TCNQ at a 12.5- $\mu\text{m}$ -radius microdisk electrode in either NB or DCE as described earlier.<sup>3,7</sup> The driving force for ET reaction was expressed as  $\Delta E^0 + \Delta_w^0\varphi$ . Although  $\Delta_w^0\varphi$  could not be found without an extrathermodynamic assumption, the difference of two reversible half-wave potentials obtained from the steady-state voltammograms of organic and aqueous redox species (with respect to the same Ag/AgCl reference electrode) is approximately equal to  $\Delta E^0 + \Delta_w^0\varphi$ .<sup>3</sup> The use of the same potential scale allowed direct comparison of our results to those in refs 3b,c and 7.

## Results and Discussion

**Concentration Dependencies of  $\Delta_w^0\varphi$ .** Depending on the phase in which the concentration of the common ion was varied, the relative  $\Delta_w^0\varphi$  value is given either by eq 5a

$$\Delta_w^0\varphi = \text{const} + S \log[\text{common ion}]_w \quad (5a)$$

or by eq 5b

$$\Delta_w^0\varphi = \text{const} + S \log[\text{common ion}]_o \quad (5b)$$

where *S* is the slope. The experimentally determined slope values are summarized in Table 1. In all cases, the  $\Delta_w^0\varphi$  vs  $\log[\text{common ion}]$  dependences were linear with high correlation coefficients (>0.99). As discussed previously,<sup>6c</sup> ZnPor is not suitable for obtaining potential dependences (i.e.,  $\Delta_w^0\varphi$  vs  $\log[\text{common ion}]_o$ ) when  $\text{ClO}_4^-$  is used as a common ion. Very small *S* values are obtained in such experiments because of extensive ion pairing between  $\text{ClO}_4^-$  and a cationic form of redox species. In contrast, using TCNQ as a redox probe, the slope values close to 59 mV/decade were obtained for both DCE and NB (Table 1). The almost Nernstian slope values obtained by varying the common ion concentration in either aqueous or organic solution indicate that ion pairing of supporting electrolyte in either phase does not affect the interfacial potential drop.

**Effect of the Common Ion Adsorption.** The adsorption of ZnPor at the ITIES recently observed by Girault's group<sup>24</sup> can be the reason for the potential-independent rate of ZnPor oxidation. To check this hypothesis, we probed the kinetics of reaction 2 with  $\text{TBA}^+$  used as a surface-active common ion (Figure 3). Reid et al.<sup>25</sup> observed rapid decrease in surface tension at the liquid/liquid interface with increasing concentration of  $\text{TBA}^+$  in aqueous phase. More recently, the adsorption of  $\text{TBA}^+$  at the water/NB interface from aqueous bromide and chloride solutions was reported by Uchiyama et al.<sup>26</sup> In our experiments, at lower concentrations of  $\text{TBA}^+$  in water (e.g.,  $[\text{TBA}^+]_w < 25$  mM), the interface formed a meniscus in the glass cell (i.e., the organic phase was convex), but at higher concentrations, the interface became flat. Moreover, at high  $[\text{TBA}^+]_w$  (i.e., >0.1 M for DCE/water and >0.2 M for NB/water), a film forms at the interface. Although the film could

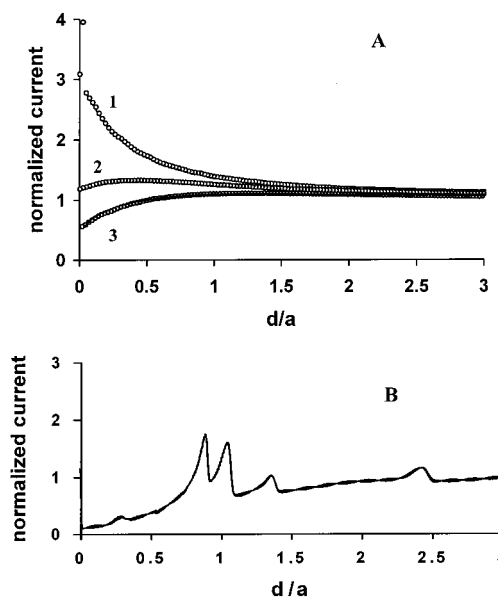


**Figure 3.** Current–distance curves for a 12.5- $\mu\text{m}$ -radius Pt tip approaching the water/DCE interface. (A) Aqueous phase contained 0.1 mM  $\text{Na}_2\text{Ru}(\text{CN})_6$ , 0.1 M NaCl, and 3.1 (1), 12.5 (2), and 50 (3) mM TBACl. DCE was 2 mM in ZnPor and 50 mM in TBAPF<sub>6</sub>. Symbols, experimental data; solid lines, theory.<sup>3a</sup> (B) Current oscillations caused by the film formation at  $[\text{TBACl}] = 100$  mM.

not be seen by the naked eye, the appearance of abnormal peaks on the current–distance curves (Figure 3B) points to the multilayer film formation at the ITIES.<sup>3b</sup> In contrast, perchlorate is not strongly adsorbed at the ITIES. Zhang et al. showed recently that the adsorption of  $\text{ClO}_4^-$  (if any) does not significantly affect the kinetics of interfacial ET.<sup>6c</sup>

The SECM approach curves obtained at different concentrations of  $\text{TBA}^+$  in the aqueous phase (Figure 3A) show the lower tip current at higher  $[\text{TBA}^+]_w$ . The apparent heterogeneous rate constants ( $k_b$ ) of reaction 2b at the DCE/water interface extracted from the approach curves using previously developed SECM theory<sup>3a</sup> exhibit strong dependence on  $[\text{TBA}^+]_w$  (Figure 4A). The apparent transfer coefficient ( $\alpha$ ) extracted from this plot is 0.56. The  $\text{TBA}^+$  adsorption at the NB/water interface was less pronounced at  $[\text{TBA}^+]_w < 50$  mM (the interfacial shape did not change greatly when the  $\text{TBA}^+$  concentration was <50 mM). Accordingly, the  $\log k_b$  vs  $[\text{TBA}^+]_w$  dependence in this concentration range was relatively weak ( $\alpha = 0.1$ ). However, the  $k_b$  value decreased markedly at higher  $[\text{TBA}^+]_w$  (Figure 4B). These findings are in a sharp contrast with the results of our previous experiments, in which the  $k_b$  of reaction 2 was independent of  $[\text{ClO}_4^-]_w$  when perchlorate was used as a common ion (see inset in Figure 1B). Since neither perchlorate nor  $\text{TBA}^+$  is expected to strongly interact with redox reactants, the major difference between  $k_b$  vs  $\Delta_w^0\varphi$  dependences observed with those common ions is likely to be due to adsorption of  $\text{TBA}^+$  at the interface. The adsorbed  $\text{TBA}^+$  species can displace ZnPor from the interfacial region, thus increasing the distance between the redox reactants and decreasing the ET rate. The specific adsorption of the bulky  $\text{TBA}^+$  (3.85 Å radius) at the ITIES should result in a thicker mixed solvent layer.<sup>27</sup> This effect may also contribute to the increase in the distance between the aqueous and organic reactants. The larger separation distance in turn increases the fraction of the interfacial voltage dropping between the aqueous and organic reactants, so that the dependence of the  $k_b$  on  $\Delta_w^0\varphi$  should appear when  $\text{TBA}^+$  is used as a common ion. Thus, the decrease in the  $k_b$  with increasing  $[\text{TBA}^+]_w$  can be caused by two concomitant and interrelated

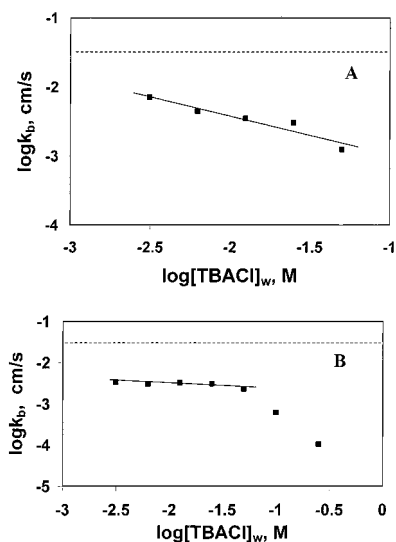


**Figure 4.** Dependence of the rate of ET between ZnPor and  $\text{Ru}(\text{CN})_6^{3-}$  on TBACl concentration in the aqueous phase. In addition to TBACl, aqueous solution contained 0.1 mM  $\text{Na}_4\text{Ru}(\text{CN})_6$  and 0.1 M NaCl. The organic phase was DCE (A) or NB (B) containing 2 mM ZnPor and 50 mM TBAPF<sub>6</sub>. Here and in other figures horizontal dashed lines show the diffusion limit for the ET rate measurements by SECM under corresponding experimental conditions.

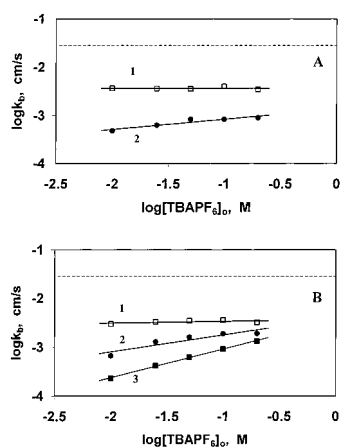


**Figure 5.** Dependence of the rate of ET between ZnPor and  $\text{Ru}(\text{CN})_6^{3-}$  on TBAPF<sub>6</sub> concentration in organic phase. The organic phase was DCE (A) or NB (B) containing 2 mM ZnPor. The aqueous phase contained 0.1 mM  $\text{Na}_4\text{Ru}(\text{CN})_6$ , 0.1 M NaCl, and 10 mM (curve 1), 50 mM (curve 2), or 100 mM (curve 3) TBACl.

effects—the increasing separation between redox species and the potential dependence of the ET rate. These two factors can be separated by probing the dependence of the rate constant on  $[\text{TBA}^+]_o$ .

#### Effect of Common Ion Concentration in Organic Phase.

In previous SECM experiments,<sup>3,6–8</sup> the concentration of the common ion in organic solvent was kept constant to avoid complications, which might be caused by changes in the diffuse layer thickness and the extent of ion pairing. As shown in Table 1,  $\Delta_w^0\varphi$  dependences on  $[\text{TBA}^+]_o$  and  $[\text{ClO}_4^-]_o$  are essentially Nernstian for both DCE/water and NB/water interfaces. Two  $\log k_b$  vs  $\log [\text{TBA}^+]_o$  dependencies obtained for reaction 2b at the water/DCE interface at  $[\text{TBA}^+]_w = 10$  mM (curve 1) and  $[\text{TBA}^+]_w = 50$  mM (curve 2) are shown in Figure 5A. While at a lower  $[\text{TBA}^+]_w$  value the ET rate is independent of  $[\text{TBA}^+]_o$  ( $\alpha = 0.0$ ), at  $[\text{TBA}^+]_w = 50$  mM the linear  $\log k_b$  vs  $\log [\text{TBA}^+]_o$  dependence can be seen ( $\alpha = 0.21$ ). At NB/water interface, the picture is even more clear—the apparent  $\alpha$  value changes from

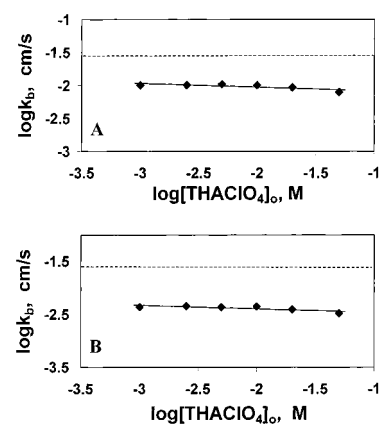


**Figure 6.** Dependence of the rate of ET between ZnPor and  $\text{Ru}(\text{CN})_6^{3-}$  on  $\text{THAClO}_4$  concentration in organic phase. The organic phase was DCE (A) or NB (B) containing 2 mM ZnPor. The aqueous phase contained 0.1 mM  $\text{Na}_4\text{Ru}(\text{CN})_6$ , 0.1 M NaCl, and 100 mM  $\text{NaClO}_4$ .

0.03 at  $[\text{TBA}^+]_w = 10$  mM (curve 1) to 0.34 at  $[\text{TBA}^+]_w = 50$  mM (curve 2) and to 0.58 at  $[\text{TBA}^+]_w = 100$  mM (curve 3).

Kakiuchi's treatment of ionic adsorption at the ITIES<sup>28</sup> is useful for understanding of these results. According to that model, at any given  $\Delta_w^0\varphi$  the adsorption of a common ion occurs either from the organic or from the aqueous side of the interface. Because the interfacial voltage was varied within a narrow range ( $\sim 100$  mV) and the experimental results point to the adsorption of  $\text{TBA}^+$  from the aqueous phase, one can expect no significant adsorption of  $\text{TBA}^+$  from organic phase under our experimental conditions. (This conclusion is also supported by essentially the same shape of the interfacial meniscus observed for a wide range of  $[\text{TBA}^+]_o$ , between 10 and 200 mM, and by the absence of a multilayer interfacial film at high  $[\text{TBA}^+]_o$ .) Thus, at low concentrations of  $\text{TBA}^+$  in water, its surface concentration is also low, and ZnPor remains adsorbed on the ITIES. Under these conditions, the ET rate constant is essentially potential-independent (curve 1 in Figure 5A,B). At higher  $[\text{TBA}^+]_w$ , ZnPor gets displaced from the interface, and the rate constant of reaction 2b depends strongly on  $[\text{TBA}^+]_o$  (curves 2 and 3 in Figure 5).

One should notice that the  $k_b$  values in Figure 5 increase with increasing  $[\text{TBA}^+]_o$ . This cannot be attributed to displacement of ZnPor from the phase boundary. Unlike the  $k_b$  vs  $[\text{TBA}^+]_w$  dependences in Figure 4, which represent the combination of the effects of ZnPor desorption and potential dependence of the ET rate, the  $k_b$  vs  $[\text{TBA}^+]_o$  dependences reflect only the effect of  $\Delta_w^0\varphi$  on the ET rate. The increase in the apparent  $\alpha$  value with  $[\text{TBA}^+]_w$  can be explained by increasing the fraction of the overall interfacial voltage dropping between ZnPor and  $\text{Ru}(\text{CN})_6^{3-}$  species. The diffuse double layer effect in water cannot be responsible for the observed increase in ET rate with  $[\text{TBA}^+]_o$  because the increase in  $[\text{TBA}^+]_o$  shifts  $\Delta_w^0\varphi$  to more negative values and causes the depletion (rather than accumulation) of negatively charged  $\text{Ru}(\text{CN})_6^{3-}$  at the interface.

Changing the electrolyte concentration in organic solution could affect the interfacial ET rate in different ways. The ion pairing effect discussed recently by Quinn and Kontturi<sup>29</sup> is less important in our system because the organic reactant (ZnPor) is a neutral species. To check the possibility that the observed potential dependence of ET rate is caused by diffuse layer effect in organic phase,<sup>30</sup> the  $\log k_b$  vs  $\log [\text{ClO}_4^-]_o$  dependences were obtained by using perchlorate as a common ion (Figure 6). Very small  $\alpha$  values (i.e., 0.05 at the DCE/water and 0.07 at the NB/water interface) extracted from Figure 6 indicate the organic diffuse layer effect on the rate of reaction 2b is negligibly small.

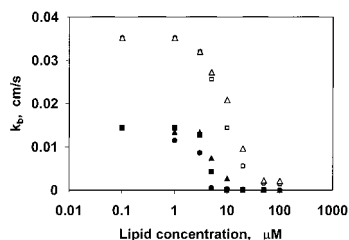


**Figure 7.** Dependence of the rate constant of ET between ZnPor<sup>+</sup> and Ru(CN)<sub>6</sub><sup>4-</sup> (filled symbols) or Fe(CN)<sub>6</sub><sup>4-</sup> (open symbols) on lipid concentration in benzene. The number of methylene groups in the lipid hydrocarbon chain was 10 (triangles), 12 (squares), and 16 (circles). The organic phase contained 0.25 M THAClO<sub>4</sub>, 0.5 mM ZnPor, and lipid. The water phase contained 0.1 M NaCl, 0.1 M NaClO<sub>4</sub>, and 7 mM Ru(CN)<sub>6</sub><sup>4-</sup> or Fe(CN)<sub>6</sub><sup>4-</sup>. Rate constants were obtained by fitting experimental approach curves to the theory.<sup>3a</sup>

#### Long-Distance ET across Phosphatidylserine Monolayers.

Similarly to the previous experiments with phosphatidylcholine (PC) lipids,<sup>3c</sup> the formation of a molecular monolayer of a long-chain phosphatidyl serine (PS) lipid impeded ET across the liquid/liquid interface. After the addition of a lipid stock solution to the organic phase, the measured rate constant decreased rapidly and within 15–20 min, reached the limiting value (corresponding to a specific concentration of lipid in organic phase). The diffusion-controlled adsorption of PS is slightly faster than PC adsorption, which required 30–40 min to come to equilibrium.<sup>3c</sup>

Several dependences of  $k_b$  vs lipid concentration obtained for two different aqueous redox species (Ru(CN)<sub>6</sub><sup>4-</sup> and Fe(CN)<sub>6</sub><sup>4-</sup>, filled and open symbols, respectively) and three different lipids [C-10 (Δ), C-12 (□), and C-16 (○)] are shown in Figure 7. As discussed earlier,<sup>3c</sup> the decrease in ET rate with increasing lipid concentration points to the increasing fraction of the interfacial area covered with lipid. At higher concentrations of any lipid (i.e.,  $\geq 50 \mu\text{M}$ ), the ET rate between Ru(CN)<sub>6</sub><sup>4-</sup> and ZnPor<sup>+</sup> across a complete monolayer of any lipid with a number of methylene groups,  $n \geq 10$ , is immeasurably slow (filled symbols in Figure 7). This shows that the lipid films are sufficiently compact to make the current through defects negligibly small under our experimental conditions. For the Ru(CN)<sub>6</sub><sup>4-</sup>/ZnPor<sup>+</sup> reaction, the effective heterogeneous rate constant can be related to the fraction of the ITIES area covered with lipid ( $\theta$ ):<sup>31,3c</sup>

$$k_f(\theta) = (1 - \theta)k_f(0) \quad (6)$$

where  $k_f(0)$  is the rate constant at the lipid-free ITIES. Thus, Figure 7 essentially represents the  $\theta$  vs [lipid] dependence, which can be fit to the Langmuir isotherm, as it was shown for PC adsorption in ref 3c.

When Ru(CN)<sub>6</sub><sup>4-</sup> is replaced with Fe(CN)<sub>6</sub><sup>4-</sup> (for which  $\Delta E^\circ$  is about 0.5 V larger), the  $k_f$  decreases markedly with increasing concentration of lipid but does not vanish at higher concentrations (open symbols in Figure 7). Instead, it reaches a limiting value at about 50  $\mu\text{M}$  and does not change at higher lipid concentrations. This saturation points to the formation of a complete phospholipid monolayer at the ITIES. In the same concentration range (i.e., [lipid]  $\geq 20 \mu\text{M}$ ), the formation of compact PS monolayers was observed previously at the water/nitrobenzene interface.<sup>20</sup>

The ET between Fe(CN)<sub>6</sub><sup>4-</sup> and ZnPor<sup>+</sup> occurs at a measurable rate via tunneling through the monolayer. Kakiuchi et al.<sup>20b</sup> reported that the differential capacity of the ITIES covered with a PS monolayer was similar to that obtained with an analogous PC lipid. They concluded that at room temperature both families of lipids form liquid-expanded monolayers at the NB/water

**TABLE 2: Rate Constants of Long-Range ET between ZnPor<sup>+</sup> and Fe(CN)<sub>6</sub><sup>4-</sup> across Phosphatidylserine (PS) and Phosphatidylcholine (PC) Monolayers Adsorbed at the BZ/Water Interface<sup>a</sup>**

PS	$k_f \times 10^3$ , cm/s	PC	$k_f \times 10^3$ , cm/s (from ref 3c)
C-10	1.9	C-10	12
C-12	1.4	C-12	4.8
C-16	0.3	C-16	1.6–6.5

<sup>a</sup> BZ contained 0.5 mM ZnPor, 0.25 M THAClO<sub>4</sub>, and 100  $\mu\text{M}$  lipid. The bottom (aqueous) phase contained 7 mM Na<sub>4</sub>Fe(CN)<sub>6</sub>, 0.1 M NaCl, and 0.1 M NaClO<sub>4</sub>.

interface. Thus, similar blocking of interfacial ET by both types of lipid films can be expected. However, the rate constants of reaction 1b across different PS monolayers turned out to be significantly lower than the rate constants across PC spacers (with the same number of methylene groups) measured under the same experimental conditions (Table 2). This cannot be explained by smaller penetration of ZnPor<sup>+</sup> into the lipid phase. If PS films were less permeable to ZnPor<sup>+</sup> than PC films, a strong distance dependence of the ET rate would be observed. On the contrary, the ET rates across a C-10 and a C-12 monolayers were almost identical (Figure 7), and the rate constant for C-16 was only  $\sim 5$  times lower than that for C-10.

Unlike phosphatidylcholines, which are neutral, phosphatidylserine lipids are negatively charged at pH 7.<sup>32</sup> The differences in ET rates across PS and PC films can be related to the repulsion of anionic Fe(CN)<sub>6</sub><sup>4-</sup> species by negatively charged heads of the PS lipid surfactants. Such a repulsion may result in both the decreased interfacial concentration of Fe(CN)<sub>6</sub><sup>4-</sup> and the larger separation of the redox reactants. The PS films can be rendered neutral by decreasing the aqueous phase pH to  $< 5$ . This should produce two opposite effects. A neutral PS film is expected to be more compact than a charged film because of lower electrostatic repulsion between lipid molecules and thus should block ET stronger. Apparently, this effect is counterbalanced by the elimination of Fe(CN)<sub>6</sub><sup>4-</sup> repulsion discussed above, and the net effect of the pH change on the ET rate is small (e.g.,  $k_b = 1.8 \times 10^{-3}$  cm/s at pH 4 vs  $2.2 \times 10^{-3}$  cm/s at pH 6.5 for a complete C-10 monolayer under the same conditions). Although this explanation is tentative, quantitative modeling of the pH effects on ET rate is problematic because the changes in film structure can also affect the extent of ZnPor penetration into the lipid layer.

The ZnPor<sup>+</sup> penetration into lipid phase prevents any quantitative analysis of the  $k_f$  vs  $n$  results in terms of a distance dependence of ET. An attempt was made to improve the blocking properties of the spacer by solidifying liquid lipid monolayers. Liquid-expanded PS monolayers formed at the ITIES at room temperature can be converted to the liquid-condensed state or even made solid by addition of a low concentration of a divalent cation (e.g., Ca<sup>2+</sup> or Mg<sup>2+</sup>).<sup>20b,33</sup> Three approach curves for the Fe(CN)<sub>6</sub><sup>4-</sup>/ZnPor ET across a C-12 monolayer in the absence (curve 1) and presence (curves 2, 3) of Ca<sup>2+</sup> in the aqueous phase are presented in Figure 8. While the lower feedback current in the presence of calcium is expected (curve 2), the increase in  $i_T$  upon addition of calcium to the aqueous phase (curve 3) is surprising. The higher value of the effective rate constant (i.e., 0.0042 cm/s from curve 3 vs 0.0014 cm/s from curve 1 in Figure 8) points to a weaker blocking effect exerted by a solidified lipid film. This observation suggests that the addition of calcium ion results in a significantly higher defect density in the lipid film. This observation is not in conflict with low values of differential capacity of PS monolayers measured in the presence of Ca<sup>2+</sup>.<sup>20b</sup>

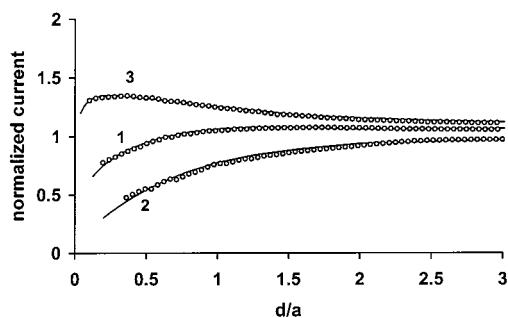


**Figure 8.** Approach curves for a full monolayer (100  $\mu\text{M}$  lipid in benzene) of C-12 in the absence (1) and presence (2, 3) of  $\text{Ca}^{2+}$  in the aqueous phase. Curves 2 and 3 were obtained with a tip approaching different areas of the interface. The effective rate constant values found from the theoretical fit (solid lines) to the experimental points (symbols) were (1) 0.0014 cm/s, (2) 0.00038 cm/s, and (3) 0.0042 cm/s. The tip approached at 1  $\mu\text{m/s}$ . Aqueous phase contained 7 mM  $\text{Na}_4\text{Fe}(\text{CN})_6$ , 0.1 M NaCl, 0.1 M  $\text{NaClO}_4$ , and 20  $\mu\text{M}$   $\text{CaCl}_2$  (2, 3). BZ was 0.5 mM in ZnPor and 0.25 M in  $\text{THAClO}_4$ .

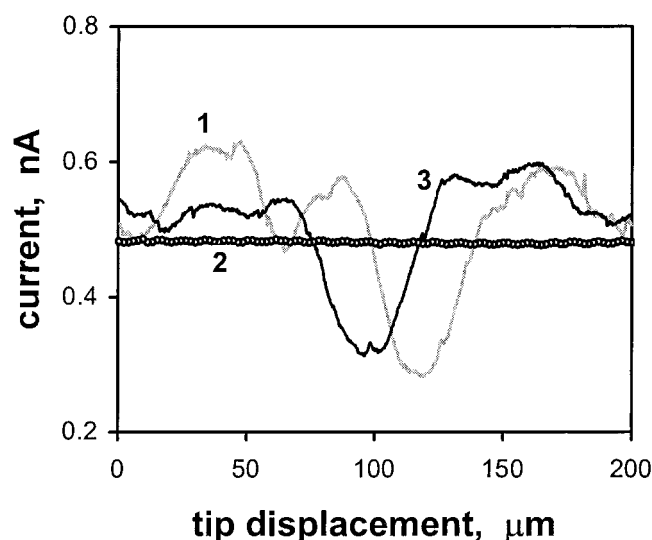


**Figure 9.** Images of the lipid films adsorbed at the BZ/water interface obtained by scanning a 12.5- $\mu\text{m}$ -radius tip along one axis parallel to the phase boundary. The ITIES was covered with a complete monolayer of PS lipid (C-10). Aqueous phase contained 10 mM  $\text{Na}_4\text{Fe}(\text{CN})_6$ , 0.1 M NaCl, and 0.1 M  $\text{NaClO}_4$ . BZ was 0.5 mM in ZnPor and 0.25 M in  $\text{THAClO}_4$ . The lipid concentration in BZ was 100  $\mu\text{M}$ . The concentration of  $\text{Ca}^{2+}$  in the aqueous phase was (1, 3) 20  $\mu\text{M}$  and (2) 0  $\mu\text{M}$ . The tip/ITIES distance was  $\sim 4$   $\mu\text{m}$ . Curves 1 (forward) and 3 (reverse) were obtained by scanning a SECM tip above the same area of the lipid film formed in the presence of calcium ion in the water phase.

Even a small number of pinholes greatly increases the ET rate across a blocking monolayer film, while the combined area of those defects (which affects the interfacial capacitance) can be very small.<sup>18b,d,31</sup>

To investigate the film uniformity, the tip was scanned above the monolayer in the  $x$ - $y$  plane parallel to the interface. (In this way micrometer-sized domains of different reactivity have previously been detected in monolayers consisting of two different lipids.<sup>3d</sup>) When the tip was scanned above the interface covered with C-10 lipid and no calcium was added to the solution, the  $i_T$  was practically constant and independent of the ( $x,y$ ) position of the tip (curve 2 in Figure 9). The interface appears to be flat and smooth. Major fluctuations of the current appeared after the addition of 20  $\mu\text{M}$  of  $\text{Ca}^{2+}$  to the aqueous layer (curve 1 in Figure 9). Two different kinds of micrometer-sized domains can be seen in curve 1 corresponding to a lower  $i_T$  (i.e., smaller  $k_f$  value) and to a higher current response (i.e.,

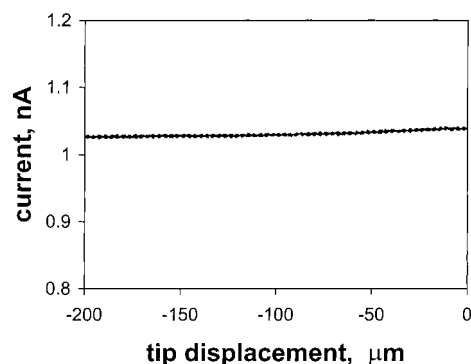


**Figure 10.** An SECM tip was scanned in the  $x$ -direction above a C-10 monolayer adsorbed at the BZ/water interface 1 h after the addition of 20  $\mu\text{M}$   $\text{Ca}^{2+}$  to the aqueous phase. Other conditions are the same as for curve 2 in Figure 9.

larger  $k_f$  value) as compared to curve 2. We take the former to correspond to domains of solidified lipid monolayer that produces a stronger blocking effect on the ET reaction. Clearly, a micrometer-sized zone, which produces a higher feedback current, cannot be completely free of lipid (if this were the case, the  $\text{Fe}(\text{CN})_6^{4-}/\text{ZnPor}$  ET reaction at such a domain would be diffusion-controlled, and the measured feedback current would be much higher). A more plausible explanation is that the pinhole defects in the monolayer are clustered within such domains. The highest feedback current in Figure 8 (curve 3) apparently corresponds to such a domain.

The stability of the domains on the phase boundary was checked by using forward (Figure 9, curve 1) and reverse (curve 3) scans at the same spot of the interface. Although the forward and reverse scans are not completely retracable and some interfacial features change on the experimental time scale ( $\sim 2$  min), the essential features of the imaged domains are reproducible. Interestingly, the distribution of defects in the monolayer depend greatly on the way those defects were nucleated. Figure 10 shows the data obtained at a PS (C-10) monolayer, which was adsorbed at the ITIES with no divalent cation present in the aqueous solution. The feedback current increased significantly after the addition of 20  $\mu\text{M}$   $\text{Ca}^{2+}$  to the water phase (cf. curve 2 in Figure 9). However, no domain structure was detected when the tip was scanned horizontally (in the  $x$ - $y$  plane) above the interface (Figure 10). Thus, the exposure of a preformed PS monolayer to calcium results in the formation of pinhole defects, which are uniformly distributed on the interface, and a consistently increased ET rate across the film.

## Conclusions

The essentially potential-independent rate of heterogeneous ET between organic ZnPor and aqueous  $\text{Fe}(\text{CN})_6^{3-}$  can be attributed to the adsorption of ZnPor at the interface. When a surface-active common ion (e.g.,  $\text{TBA}^+$ ) is added to the system, it can displace ZnPor from the interface. Under these conditions, the ET rate exhibits strong dependence on the interfacial potential ( $\Delta_w^0\varphi$ ). The desorption of ZnPor apparently increases the fraction of the interfacial voltage dropping between the reactants and in this way increases the potential dependence of the ET rate. A strong dependence of  $k_b$  on  $\Delta_w^0\varphi$  observed for ET involving neutral redox species dissolved in the organic phase suggests that the potential drop across a mixed-solvent layer may be larger than the few millivolt value suggested previously.<sup>14</sup>

Long-range ET was probed across 1,2-diacyl-*sn*-glycero-3-phospho-L-serine monolayers. The blocking properties of these

films turned out to be similar to those previously reported for phosphatidylcholine monolayers.<sup>3c</sup> A relatively weak distance dependence of ET rate points to partial penetration of ZnPor<sup>+</sup> into the lipid monolayer. An attempt to solidify phosphatidylserine films by adding calcium ions to the aqueous phase resulted in a formation of two types of domains in the monolayer. Although micrometer-sized domains in lipid monolayers often form under the increased surface pressure and also in the mixed films, the observation of a domain structure in a monolayer formed from a single lipid at the ITIES is not common. The properties of the film depend dramatically on the adsorption conditions, thus indicating the importance of nucleation phenomena for the formation of the domains.

**Acknowledgment.** The support by the donors of the Petroleum Research Fund administrated by the American Chemical Society, NSF Division of International Programs, and a grant from PSC-CUNY are gratefully acknowledged. The software for SECM measurements was generously provided by Prof. D. O. Wipf (Mississippi State University).

## References and Notes

- (1) *Liquid Interfaces in Chemical, Biological, and Pharmaceutical Applications*; Volkov, A. G., Ed.; Marcel Dekker: New York, 2001.
- (2) (a) Amemiya, S.; Ding, Z.; Zhou, J.; Bard, A. *J. Electroanal. Chem.* **2000**, *483*, 7. (b) Barker, A. L.; Gonsalves, M.; Unwin, P. R. *Anal. Chim. Acta* **1999**, *385*, 223. (c) Mirkin, M. V.; Tsionsky, M. In *Scanning Electrochemical Microscopy*; Bard, A. J., Mirkin, M. V., Eds.; Marcel Dekker: New York, 2001; p 299.
- (3) (a) Wei, C.; Bard, A. J.; Mirkin, M. V. *J. Phys. Chem.* **1995**, *99*, 16 033. (b) Tsionsky, M.; Bard, A. J.; Mirkin, M. V. *J. Phys. Chem.* **1996**, *100*, 17 881. (c) Tsionsky, M.; Bard, A. J.; Mirkin, M. V. *J. Am. Chem. Soc.* **1997**, *119*, 10 785. (d) Delville, M.-H.; Tsionsky, M.; Bard, A. J. *Langmuir* **1998**, *14*, 2774.
- (4) Solomon, T.; Bard, A. J. *Anal. Chem.* **1995**, *67*, 2787.
- (5) Selzer, Y.; Mandler, D. *J. Electroanal. Chem.* **1996**, *409*, 15.
- (6) (a) Barker, A. L.; Macpherson, J. V.; Unwin, P. R. *J. Phys. Chem. B* **1998**, *102*, 1586. (b) Zhang, J.; Unwin, P. R. *J. Phys. Chem. B* **2000**, *104*, 2341. (c) Zhang, J.; Barker, A. L.; Unwin, P. R. *J. Electroanal. Chem.* **2000**, *483*, 95. (d) Barker, A. L.; Unwin, P. R.; Bard, A. J. *J. Phys. Chem. B* **1999**, *103*, 7260.
- (7) Liu, B.; Mirkin, M. V. *J. Am. Chem. Soc.* **1999**, *121*, 8352.
- (8) Ding, Z.; Quinn, B. M.; Bard, A. J. *J. Phys. Chem. B* **2001**, *105*, 6367.
- (9) Zhang, Z.; Yuan, Y.; Sun, P.; Su, B.; Guo, J.; Shao, Y.; Girault, H. H. *J. Phys. Chem. B*, in press.
- (10) (a) Marcus, R. A. *J. Phys. Chem.* **1990**, *94*, 1050. (b) Marcus, R. A. *J. Phys. Chem.* **1990**, *94*, 4152. (c) Marcus, R. A. *J. Phys. Chem.* **1991**, *95*, 2010.
- (11) (a) Geblewicz, G.; Schiffrin, D. J. *J. Electroanal. Chem.* **1988**, *244*, 27. (b) Cunnane, V. J.; Schiffrin, D. J.; Beltran, C.; Geblewicz, G.; Solomon, T. *J. Electroanal. Chem.* **1988**, *247*, 203. (c) Cheng, Y.; Schiffrin, D. J. *J. Electroanal. Chem.* **1991**, *314*, 153.
- (12) Cai, C.; Mirkin, M. V., unpublished results.
- (13) Fermin, D. J.; Ding, Z.; Duong, H. D.; Brevet, P.-F.; Girault, H. H. *J. Phys. Chem. B* **1998**, *102*, 10334.
- (14) (a) Girault, H. H.; Schiffrin, D. J. *J. Electroanal. Chem.* **1988**, *244*, 15. (b) Katano, H.; Maeda, K.; Senda, M. *J. Electroanal. Chem.* **1995**, *396*, 391. (c) Schmickler, W. *J. Electroanal. Chem.* **1997**, *428*, 123.
- (15) Hanzlik, J.; Hovorka, J.; Samec, Z.; Toma, S. *Collect. Czech. Chem. Commun.* **1988**, *53*, 903.
- (16) Ding, Z.; Fermin, D. J.; Brevet, P.-F.; Girault, H. H. *J. Electroanal. Chem.* **1998**, *458*, 139.
- (17) (a) *Long-Range Electron-Transfer in Biology*; Palmer, G. A., Ed; Structure and Bonding 75; Springer-Verlag: Berlin, 1991. (b) Lahiri, J.; Fate, G. D.; Ungashe, S. B.; Groves, J. T. *J. Am. Chem. Soc.* **1996**, *118*, 2347.
- (18) (a) Chidsey, C. E. D. *Science* **1991**, *251*, 919. (b) Finklea, H. O. In *Electroanalytical Chemistry*; Bard, A. J., Ed.; Marcel Dekker: New York, 1996; Vol. 19, p 109. (c) Sachs, S. B.; Dudek, S. P.; Hsung, R. P.; Sita, L. R.; Smalley, J. F.; Newton, M. D.; Feldberg, S. W.; Chidsey, C. E. D. *J. Am. Chem. Soc.* **1997**, *119*, 10563. (d) Miller, C. J. In *Physical Electrochemistry: Principles, Methods, and Applications*; Rubinstein, I., Ed.; Marcel Dekker: New York, 1995; p 27.
- (19) (a) Finklea, H. O.; Liu, L.; Ravenscroft, M. S.; Punturi, S. *J. Phys. Chem.* **1996**, *100*, 18 852. (b) Slowinski, K.; Chamberlain, R. V.; Miller, C. J.; Majda, M. *J. Am. Chem. Soc.* **1997**, *119*, 11 910. (c) Slowinski, K.; Fong, H. K. Y.; Majda, M. *J. Am. Chem. Soc.* **1999**, *121*, 7257.
- (20) (a) Kakiuchi, T. In *Liquid-Liquid Interfaces. Theory and Methods*; Volkov, A. G.; Deamer, D. W., Eds; CRC Press: Boca Raton, FL, 1996; p 317. (b) Kakiuchi, T.; Kondo, T.; Senda, M. *Bull. Chem. Soc. Jpn.* **1990**, *63*, 3270.
- (21) Krause, R. A.; Violette, C. *Inorg. Chim. Acta* **1986**, *113*, 161.
- (22) Shao, Y.; Mirkin, M. V.; Rusling, J. F. *J. Phys. Chem. B* **1997**, *101*, 3202.
- (23) Wipf, D. O.; Bard, A. J. *J. Electrochem. Soc.* **1991**, *138*, 489.
- (24) Girault, H. H., unpublished results.
- (25) Reid, J. D.; Melroy, O. R.; Buck, R. P. *J. Electroanal. Chem.* **1983**, *147*, 71.
- (26) Uchiyama, Y.; Kitamori, T.; Sawada, T. *Langmuir* **2000**, *16*, 6597.
- (27) Girault, H. H. *Electrochim. Acta* **1987**, *32*, 383.
- (28) Kakiuchi, T. *J. Electroanal. Chem.* **2001**, *496*, 137.
- (29) Quinn, B.; Kontturi, K. *J. Electroanal. Chem.* **2000**, *483*, 124.
- (30) Pereira, C. M.; Silva, F.; Sousa, M. J.; Kontturi, K.; Murtomäki, L. *J. Electroanal. Chem.* **2001**, *509*, 148.
- (31) (a) Amatore, C.; Savéant, J. M.; Tessier, D. *J. Electroanal. Chem.* **1983**, *147*, 39. (b) Forouzan, F.; Bard, A. J.; Mirkin, M. V. *Isr. J. Chem.* **1997**, *37*, 155.
- (32) Seimiya, T.; Ohki, S. *Biochim. Biophys. Acta* **1973**, *298*, 546.
- (33) Ohnishi, S.; Ito, T. *Biochemistry* **1974**, *13*, 881.